

Very stable superoxide radical adducts of 5-ethoxycarbonyl-3,5-dimethyl-pyrroline *N*-oxide (3,5-EDPO) and its derivatives

Klaus Stolze^a, Natascha Rohr-Udilova^a, Thomas Rosenau^b,
Roswitha Stadtmüller^a, Hans Nohl^{a,*}

^aResearch Institute of Biochemical Pharmacology and Toxicology, University of Veterinary Medicine Vienna, Veterinärplatz 1, A-1210 Vienna, Austria

^bDivision of Organic Chemistry, University of Natural Resources and Applied Life Sciences (BOKU), Department of Chemistry, Muthgasse 18, A-1190 Vienna, Austria

Received 14 December 2004; accepted 31 January 2005

Abstract

Oxygen radicals are involved in the onset of many diseases. Adequate spin traps are required for identification and localisation of free radical formation in biological systems. Superoxide spin adducts with half-lives up to 20 min at physiological pH have recently been reported to be formed from derivatives of the spin trap 5-ethoxycarbonyl-5-methyl-1-pyrroline *N*-oxide (EMPO). This is a major improvement over DMPO ($t_{1/2}$ ca. 45 s), and even DEPMPO ($t_{1/2}$ ca. 14 min). In this study, an additional methyl group was introduced into position 3 or 4 of the pyrroline ring which greatly increases the stability of the respective superoxide spin adducts. In addition, the ethoxy group of EMPO was exchanged by either a propoxy- or an *iso*-propoxy group in order to test the influence of increasing lipophilic properties of the investigated spin traps. The structure of all compounds was confirmed by ¹H and ¹³C-NMR with full signal assignment. In comparison with EMPO ($t_{1/2}$ ca. 8 min) or DEPMPO ($t_{1/2}$ ca. 14 min), the superoxide adducts of all novel spin traps were considerably higher ($t_{1/2}$ ca. 12–55 min). In addition, various other spin adducts obtained from oxygen-centered as well as carbon-centered radicals (e.g. derived from methanol or linoleic acid hydroperoxide) were also detected.

© 2005 Elsevier Inc. All rights reserved.

Keywords: Spin traps; EPR; EMPO derivatives; Superoxide; Linoleic acid hydroperoxide; Free radicals

1. Introduction

Derivatives of the spin trap EMPO (5-ethoxycarbonyl-5-methyl-1-pyrroline *N*-oxide) have recently been described by several authors to be superior to the parent compound itself [1–3]. Compounds having bulky alkoxy carbonyl substituents formed considerably more stable superoxide

adducts ($t_{1/2}$ = 15–25 min [1,3]) as compared to the structurally related spin traps DMPO ($t_{1/2}$ < 1 min [4]), EMPO ($t_{1/2}$ ca. 8 min [5–7]), or even DEPMPO ($t_{1/2}$ ca. 14 min [8–10]). Since the observed spin adduct stabilisation was obviously not only due to the electron-withdrawing effect, but also due to steric influences of the alkoxy carbonyl group, it was expected that the incorporation of an additional methyl group at position 3 or 4 of the pyrroline ring of EMPO derivatives might cause increased steric shielding and thus lead to an even higher stability of the superoxide adducts.

Preliminary experiments on trapping of radicals derived from peroxidized linoleic acid using different spin traps, such as DMPO [11], DEPMPO [9,10], EMPO [7] or Trazon [12,13], have recently been reported, although an optimal spin trap for the detection of all types of oxygen- and carbon-centered radicals has not yet been found.

Aim of the present work was the synthesis of a series of 3,5- or 4,5-dimethylated pyrroline derivatives with differ-

Abbreviations: DEPMPO, 5-(diethoxyphosphoryl)-5-methyl-1-pyrroline *N*-oxide; DMPO, 5,5-dimethylpyrroline *N*-oxide; DTPA, diethylenetriaminepentaacetic acid; 3,5-EDPO, 5-(ethoxycarbonyl)-3,5-dimethyl-1-pyrroline *N*-oxide; 4,5-EDPO, 5-(ethoxycarbonyl)-4,5-dimethyl-1-pyrroline *N*-oxide; 3,5-DIPPO, 3,5-dimethyl-5-(*iso*-propoxycarbonyl)-1-pyrroline *N*-oxide; 4,5-DIPPO, 4,5-dimethyl-5-(*iso*-propoxycarbonyl)-1-pyrroline *N*-oxide; 3,5-DPPO, 3,5-dimethyl-5-(propoxycarbonyl)-1-pyrroline *N*-oxide; 4,5-DPPO, 4,5-dimethyl-5-(propoxycarbonyl)-1-pyrroline *N*-oxide; EMPO, 5-(ethoxycarbonyl)-5-methyl-1-pyrroline *N*-oxide; EPR, electron paramagnetic resonance; HFS, hyperfine splitting; LO[•], lipoxyl radical; NMR, nuclear magnetic resonance; O₂^{•-}, superoxide anion radical; SOD, superoxide dismutase

* Corresponding author. Tel.: +43 1 25077 4400; fax: +43 1 25077 4490.

E-mail address: hans.nohl@vu-wien.ac.at (H. Nohl).

ent lipophilic properties for the detection of superoxide and other radicals in aqueous solution as well as within lipid membranes.

2. Materials and methods

2.1. Chemicals

2-Bromopropionyl bromide, crotonaldehyde, linoleic acid, methacrolein, superoxide dismutase and xanthine oxidase were commercially available from Sigma–Aldrich. Petroleum ether (high boiling, 50–70 °C) was obtained from Fluka, all other chemicals from Merck.

2.2. Syntheses

Synthesis and characterization of the compounds were performed as reported earlier [1,7], in analogy to the synthesis of EMPO and its derivatives [5,6] with minor adaptations as given below.

2.2.1. Alkyl 2-bromopropionate

2-Bromopropionyl bromide (70 mmol) was slowly added to a solution of the respective alcohol (100 mmol) and pyridine (70 mmol) in CHCl_3 at 0 °C (ice bath). After stirring for 1 h, the reaction mixture was successively washed with water (50 mL), sulfuric acid (10%, 50 mL) and concentrated aqueous Na_2CO_3 (50 mL), and dried over Na_2SO_4 overnight. Solvent and excess alcohol were removed under reduced pressure. The crude, nearly colorless product was used without further purification.

2.2.2. Alkyl 2-nitropropionate

The respective alkyl 2-bromopropionate (60 mmol) was added under stirring to a solution of sodium nitrite (7.2 g,

104 mmol) and phloroglucinol dihydrate (8.5 g, 52 mmol) in dry dimethylformamide (120 mL) at room temperature. The solution was stirred overnight, poured into ice water (240 mL), and extracted four times with ethyl acetate/petroleum ether ($v/v = 4:1$, 100 mL). The combined extracts were treated twice with 100 mL of saturated Na_2CO_3 solution and dried over Na_2SO_4 . After removal of the solids by filtration, the solvent was evaporated in vacuo. The obtained colorless or pale yellow products were used further without purification.

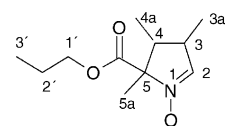
2.2.3. Alkyl 2,3-dimethyl-4-formyl-2-nitro-butanoate and alkyl 2,4-dimethyl-4-formyl-2-nitro-butanoate

23 mmol of the respective alkyl 2-nitropropionate was dissolved in a mixture of acetonitrile (10 g, 244 mmol) and triethylamine (0.2 g, 2 mmol). Crotonaldehyde (2.5 g, 38 mmol: for the 4-methyl derivatives) or methacrolein (2.5 g, 38 mmol: for the 3-methyl derivatives) was slowly added at 0 °C. The solution was stirred at room temperature overnight and then poured into a solution of ice-cold HCl (5 mL concentrated HCl in 150 mL water). The solution was extracted three times with CH_2Cl_2 and dried over anhydrous Na_2SO_4 . After filtration the mixture was distilled under reduced pressure, and the purity of the obtained product was assessed by thin layer chromatography and IR spectroscopy. If necessary, the product was re-purified by column chromatography.

2.2.4. Synthesis of the N-oxides

Synthesis of the nitrones was performed according to the procedure described previously for the synthesis of EMPO derivatives [1,7]. To a solution of the respective alkyl dimethyl-4-formyl-2-nitrobutanoate (25 mmol) in $\text{H}_2\text{O}/\text{CH}_3\text{OH}$ ($v/v = 3:2$, ca. 250 mL) an aqueous NH_4Cl solution (1.87 g in 8 mL water) was added. The mixture was carefully kept at room temperature while 8.5 g (130 mmol)

Table 1
 ^{13}C NMR data (ppm) of the spin traps



	$^2\text{C}=\text{N}$	^3C	^{3a}C	^4C	^{4a}C	^5C	COO	^1C	^2C	^3C	$^{5a}\text{CH}_3$
EMPO*	134.9	25.4	–	31.9	–	78.5	169.3	61.7	13.4	–	20.3
c-3,5EDPO	138.8	33.3	18.6	40.1	–	79.6	170.1	62.2	13.9	–	21.3
t-3,5EDPO	139.8	33.3	18.6	41.5	–	79.6	169.8	62.2	13.9	–	21.7
c-4,5EDPO	135.6	33.8	–	40.7	19.9	82.0	168.1	61.9	14.0	–	14.7
t-4,5EDPO	133.8	34.4	–	36.8	15.3	82.0	170.0	62.0	13.9	–	14.7
t-3,5DPPO	139.7	33.2	18.5	41.5	–	79.6	169.8	67.5	21.68	10.1	21.66
c-4,5DPPO	135.9	33.9	–	40.8	19.9	82.2	168.2	67.5	21.7	10.3	14.7
t-4,5DPPO	134.1	34.5	–	36.9	15.4	82.1	170.0	67.6	21.7	10.2	14.7
c-3,5DIPPO	139.5	33.3	18.5	40.1	–	79.6	169.5	69.9	21.2	–	21.3
t-3,5DIPPO	139.8	33.2	18.5	41.5	–	79.6	169.2	69.8	21.3	–	21.7
									21.4		
c-4,5DIPPO	135.7	34.0	–	41.0	20.0	82.1	168.3	70.1	21.7	–	14.8
t-4,5DIPPO	134.2	34.6	–	37.0	15.5	82.1	169.5	70.0	21.7	–	14.8

zinc dust was slowly added within 30 min. The mixture was stirred for several hours at room temperature, the white precipitate and the remaining zinc powder were removed by filtration, and the residue was washed five times with methanol (30 mL). The liquid phase was concentrated to about 10 mL and extracted four times with CH_2Cl_2 (60 mL). The organic phase was dried over Na_2SO_4 , filtered and concentrated.

2.2.5. Purification and separation of the different stereoisomers

The crude products were purified chromatographically in two steps, first on silica gel using a petroleum ether/ethanol gradient, followed by a final purification immediately before the EPR experiments on 1 mL solid phase extraction columns using a Chromabond C-18 100 mg column obtained from Macherey-Nagel (Düren, Germany).

In this way pure colourless products were obtained from all investigated spin traps. In the case of 3,5-EDPO the two possible diastereomeric products could be separated into the *cis*- and *trans*-forms. From 3,5-DPPO and 3,5-DIPPO the pure *trans*-form and very small amounts of the *cis*-form (ca. 95% pure) were obtained. 4,5-EDPO, -DPPO and -DIPPO could, however, not be separated into the *trans*- and

cis-forms. The purity of the obtained products was assessed by TLC and UV spectroscopy. Final identification of the purified products was performed by ^1H NMR, ^{13}C NMR, and IR spectroscopy (see Tables 1–3).

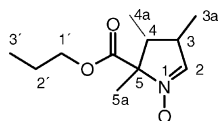
2.2.6. Preparation of lipid hydroperoxides

Linoleic acid hydroperoxide was synthesized according to O'Brien [14]. Briefly, linoleic acid was air-oxidized for 72 h in the dark at room temperature. The oxidation mixture was dissolved in petroleum ether (boiling range 60–90 °C) and extracted four times with water/methanol (v/v = 1:3). The obtained methanolic phase was counter-extracted four times with petroleum ether (boiling range 60–90 °C) and evaporated under reduced pressure. The obtained hydroperoxide was dissolved in ethanol and stored in liquid nitrogen. The concentration of hydroperoxide was determined by UV spectroscopy based on an extinction coefficient of $\epsilon_{233\text{ nm}} = 25,250\text{ M}^{-1}\text{ cm}^{-1}$ in ethanol [14].

2.3. Instruments

UV–vis spectra were recorded on Hitachi 150–20 and U-3300 spectrophotometers in double-beam mode against a blank of the respective solvent. Determination of the

Table 2
 ^1H NMR data (ppm) of the spin traps



	$^2\text{CH}=\text{N}$	$^3\text{CH}_x$	$^3\text{aCH}_3$	$^4\text{CH}_x$	$^4\text{aCH}_3$	$^1\text{CH}_x$	$^2\text{CH}_x$	$^3\text{CH}_x$	$^5\text{aCH}_3$
EMPO*	6.97t	2.75m	–	2.16m 2.60m	–	4.26m	1.31t	–	1.72s
c-3,5EDPO	6.85d	3.10m	1.25d	ci2.17dd tr2.40dd	–	4.27m	1.32t	–	1.71s
t-3,5EDPO	6.91d	3.15m	1.20d	ci2.76dd tr1.70dd	–	4.25m	1.29t	–	1.73s
c-4,5EDPO	7.03t	2.40m 2.72m	–	2.48m	1.11d	4.26m	1.31t	–	1.67s
t-4,5EDPO	6.92t	2.26m 2.94m	–	2.87m	1.12d	4.27m	1.31t	–	1.58s
t-3,5DPPO	6.91d	3.15dsx	1.21d	ci2.77dd tr1.71m	–	4.15m	1.71sx	0.95t	1.73s
c-4,5DPPO	7.06t	2.40m 2.72m	–	2.47m	1.11d	4.16m	1.70sx	0.96t	1.68s
t-4,5DPPO	6.95t	2.26m 2.95m	–	2.89m	1.12d	4.16m	1.70sx	0.95t	1.58s
c-3,5DIPPO	6.92d	3.09m	1.25d	ci2.13dd tr2.40dd	–	5.09sp	1.29d	–	1.69s
t-3,5DIPPO	6.90d	3.14dsx	1.20d	ci2.77dd tr1.69dd	–	5.06sp	1.25d	–	1.71s
c-4,5DIPPO	7.06t	2.37m 2.70m	–	2.45m	1.12d	5.10sp	1.29d	–	1.66s
t-4,5DIPPO	6.92t	2.24m 2.93m	–	2.87m	1.11d	5.10sp	1.28d	–	1.56s

Abbreviations: s, singlet; d, doublet; t, triplet; sx, sextet; sp, septet; m, multiplet; dd, doublet of doublets; dsx, doublet of sextets; ci, *cis* to ester; tr, *trans* to ester.

Table 3
IR data (cm⁻¹) of the spin traps

EMPO ^a	2985	2940	2874	1741	1582	1464	1446	1377	1341	1288	1236	1182	1107	1024	950	926	862	796	633
c-3,5EDPO	2977	2937	2876	1741	1578	1453	1446	1379	1317	1282	1228	1150	1108	1020	967	942	860	837	651
t-3,5EDPO	2975	2937	2875	1741	1577	1458	1445	1377	1303	1233	1207	1158	1109	1020	966	938	859	829	636
4,5EDPO	2977	2940	2878	1740	1578	1465	1445	1386	1369	1277	1259	1184	1122	1096	1001	929	862	803	669
t-3,5DPPO	2968	2939	2878	1742	1578	1456	1445	1377	1353	1301	1283	1206	1162	1035	954	927	910	870	636
4,5DPPO	2968	2940	2879	1741	1578	1465	1445	1387	1349	1321	1277	1183	1121	1057	1000	976	953	908	667
c-3,5DIPPO	2980	2938	2877	1741	1578	1453	1445	1376	1353	1292	1224	1157	1104	1031	968	951	908	870	634
t-3,5DIPPO	2980	2938	2875	1740	1577	1457	1445	1376	1355	1302	1283	1210	1164	1034	967	948	910	870	636
4,5DIPPO	2980	2938	2879	1735	1578	1466	1385	1376	1350	1280	1261	1184	1145	1022	1000	941	906	892	665

Intensities: strong (1741), medium (1446), weak (950).

concentrations was done measuring the absorption maxima in the range between 200 and 350 nm. IR spectra were recorded as film on an ATI Mattson Genesis Series FTIR spectrometer.

For EPR experiments Bruker spectrometers (ESP300E and EMX) were used, operating at 9.7 GHz with 100 kHz modulation frequency, equipped with a rectangular TE₁₀₂ or a TM₁₁₀ microwave cavity.

¹H NMR spectra were recorded at 300.13 MHz, ¹³C NMR spectra at 75.47 MHz on a Bruker Avance. CDCl₃ containing tetramethylsilane (TMS) as the internal standard was used as the solvent throughout. ¹³C peaks were assigned by means of APT (attached proton test), ¹H-detected heteronuclear multiple-quantum coherence (HMQC) and heteronuclear multiple bond connectivity (HMBC) spectra. A complete set of ¹H, H–H correlated, ¹³C, HMQC and HMBC spectra was recorded for each compound. All chemical shift data are given in ppm units.

3. Results

3.1. Structure of the spin traps

The identity of the synthesized spin traps was established unambiguously by NMR. In the current compound series, an additional substituent at either C-3 or C-4 was present, which could be configured either *trans* (E) or *cis* (Z) with regard to the bulky alkoxy carbonyl substituent at C-5, so that two diastereomers of each spin trap were obtained, a *cis*-compound and the respective *trans*-isomer.

The carbon NMR data of the spin traps clearly reflected the substitution pattern at the pyrroline system. The four signals of the carbons C-2 to C-5 in the heterocyclic ring appeared at averaged values of 139, 33, 41 and 80 ppm for the 3,5,5-trisubstituted derivatives, and at 135, 34, 37 (*trans*)/41 (*cis*) and 82 ppm, for the 4,5,5-trisubstituted derivatives, respectively. Substitution site and configuration had no influence on the shifts of the carboxyl carbon and the alkoxy moieties. In contrast, the 5a-methyl group gave a resonance at about 21.5 ppm for 3,5,5-trisubstituted and at 14.7 ppm for 4,5,5-trisubstituted compounds. Due to this pronounced shift difference, the 5a-CH₃ signal can serve as a quick indicator as to the presence of a 3,5,5-substituted or 4,5,5-substituted compound.

In the 3,5,5-trisubstituted derivatives, the *cis/trans*-configuration had no influence on C-3, and only a small effect on C-4: the C-4 in the *trans*-compounds showed a weak downfield shift of about 1.4 ppm relative to the *cis*-counterpart. In contrast, in the 4,5,5-trisubstituted derivatives the difference between the two diastereomers was much larger. C-4 in the *trans*-compounds experienced a strong highfield shift by 4 ppm relative to the *cis*-compound, and C-3 a 0.6 ppm downfield shift. These data reflect that 3- and 5-substituents in the pyrrolidine are positioned relatively remote from each other, whereas 4- and 5-substituents

are placed in close proximity showing strong interactions. This was also seen by the shift values of the 3a- and 4a-methyl groups; 3a-CH₃ appeared at 18.5 ppm independent of the configuration, whereas the 4a-CH₃ moiety gave resonances at 20 ppm in *cis*-compounds and at 15.4 ppm in *trans*-derivatives.

Also the ¹H NMR data fully agreed with the expectations. The H-2 appeared as doublet in the case of 3-substituted derivatives. In 4-substituted compounds, H-2 showed a triplet – not a doublet of doublets, indicating similar coupling constants to the geminal H-3 protons. 3a-CH₃ substituents were found at 1.25 ppm for *cis*-derivatives and at 1.20 ppm for the *trans*-compounds, 4a-CH₃ groups resonated more up-field at about 1.12 ppm independent of the configuration. The 5a-CH₃ group was found at approx. 1.70 ppm in 3,5,5-trisubstituted pyrrolines with almost no difference between *cis*- and *trans*-isomers, whereas in the 4,5,5-trisubstituted counterparts there was an obvious influence of the configuration, with the 5a-CH₃-resonance of the *cis*-isomer (1.67 ppm) being shifted 0.1 ppm downfield relative to the *trans*-isomer (1.57 ppm).

An interesting feature of the ¹H spectra were the signal patterns of the H-3 and H-4 protons, which showed significantly different patterns according to both substitution site and configuration. In 3,5,5-derivatives, the proton at C-3 appeared at around 3.10 ppm, and the shift difference between *cis*- and *trans*-isomers was rather small (0.05 ppm). The two geminal H-4 protons appeared at about 2.15 ppm/2.40 ppm for the *cis*-compound and 1.70 ppm/2.76 ppm for the *trans*-compound. Thus, the shift difference between these two protons was much more pronounced for the *trans*-isomers – more than 1 ppm. In the *trans*-3,5-derivative, the highfield proton (1.70 ppm) is configured *cis* to both methyl groups at C-3 and C-4 and *trans* to the alkoxy carbonyl moiety at C-5, the downfield proton (2.76 ppm) is consequently placed *trans* to both methyl groups and *cis* to the ester. In the *cis*-3,5-derivative, the situation is reversed: the highfield proton (2.15 ppm) is now configured *trans* to the two vicinal methyl groups at C-3 and C-4 and *cis* to the ester, the downfield proton (2.40 ppm) is in *cis*-arrangement to the methyl groups and *trans* to the ester.

In the 4,5,5-trisubstituted pyrroline derivatives, the resonance of H-4 was found at 2.46 ppm for the *cis*-isomers and at 2.88 ppm for the *trans*-isomers. H-4 was thus found more upfield than H-3 in the 3,5,5-compounds, and there was also a clear difference between the *cis*- and *trans*-derivatives. The two geminal H-3 protons appeared at 2.40 ppm/2.72 ppm for the *cis*-compound and at 2.26 ppm/2.94 ppm for the *trans*-compound. In analogy to the 3,5,5-derivatives, the shift differences between the two geminal ring protons was more pronounced for the *trans*-isomer. In the *trans*-4,5-compounds, the highfield proton (2.26 ppm) is placed *cis* to the methyl at C-4 (*trans* to the ester), the downfield proton (2.94 ppm) is consequently in *trans*-configuration relative to 4a-CH₃ (*cis* to the

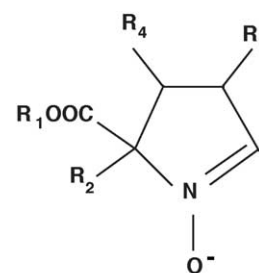
ester). In the *cis*-4,5-derivative, the highfield proton (2.40 ppm) is now configured *trans* to 4-CH₃, (*cis* to the ester), the downfield proton (2.72 ppm) consequently *cis* to 4-CH₃ and *trans* to the ester. The resonances of the alkoxy moieties fell in the expected ranges, the 1'-methylene groups in the ethoxy and propoxy residues showed pronounced diastereotopic splitting. The respective NMR data are summarized in Tables 1 and 2.

IR spectra of the different compounds show characteristic differences especially in the so-called fingerprint range around 1000 cm⁻¹. In this way the different fractions obtained from the chromatography columns could be pre-selected before NMR characterization.

The respective IR data are summarized in Table 3.

3.2. Spin trapping of superoxide radicals

The general structure of the spin traps is shown in Fig. 1. In Fig. 2(a), the EPR spectrum of the superoxide adduct of *trans*-3,5-EDPO is given as an example. The adduct was generated in the xanthine/xanthine oxidase system at pH 7.4. No EPR spectrum was observed in the presence of SOD (Fig. 2(b)). Under these conditions similar EPR spectra were obtained from *trans*-3,5-DPPO and *trans*-3,5-DIPPO (not shown). The superoxide adduct of the diastereomeric *cis*-3,5-EDPO, on the other hand, could be readily distinguished due to its characteristically different spectral parameters (Fig. 2(c)) and considerably lower stability (*t*_{1/2} = 11.5 min) as compared to the *trans*-compound (*t*_{1/2} = 44.2 min). The remarkable line-width difference between the *cis*- and the *trans*-form is probably due to stereochemically sensitive contributions of the unresolved methyl protons. The respective *cis*-isomers



EMPO:	R ₁ = C ₂ H ₅	R ₂ = CH ₃	R ₃ = H	R ₄ = H
3,5-EDPO:	R ₁ = C ₂ H ₅	R ₂ = CH ₃	R ₃ = CH ₃	R ₄ = H
4,5-EDPO:	R ₁ = C ₂ H ₅	R ₂ = CH ₃	R ₃ = H	R ₄ = CH ₃
3,5-DPPO:	R ₁ = C ₃ H ₇	R ₂ = CH ₃	R ₃ = CH ₃	R ₄ = H
4,5-DPPO:	R ₁ = C ₃ H ₇	R ₂ = CH ₃	R ₃ = H	R ₄ = CH ₃
3,5-DIPPO:	R ₁ = <i>iso</i> -C ₃ H ₇	R ₂ = CH ₃	R ₃ = CH ₃	R ₄ = H
4,5-DIPPO:	R ₁ = <i>iso</i> -C ₃ H ₇	R ₂ = CH ₃	R ₃ = H	R ₄ = CH ₃

Fig. 1. General structure of the spin traps.

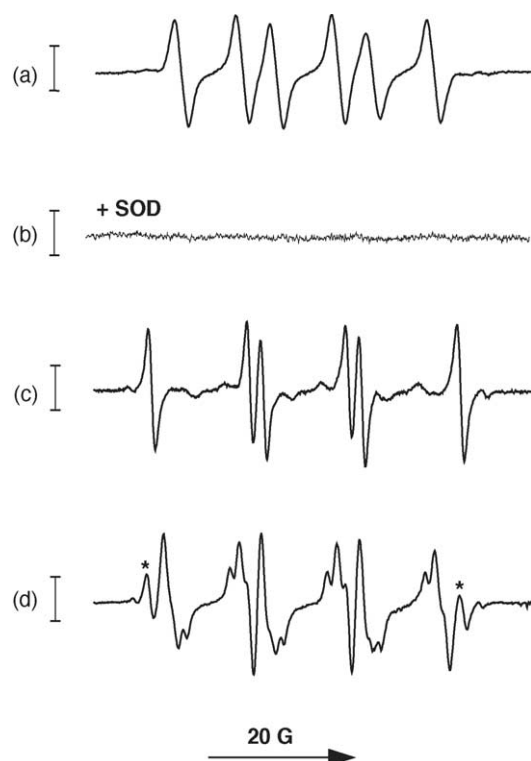


Fig. 2. Formation of the superoxide adducts of the spin traps *trans*-3,5-EDPO, *cis*-3,5-EDPO, and *cis/trans*-4,5-EDPO; (a) *Trans*-3,5-EDPO (20 mM), catalase (250 U/mL), xanthine (0.2 mM) and xanthine oxidase (50 mU/mL) in oxygenated phosphate buffer (20 mM, pH 7.4, containing 0.4 mM DTPA) were incubated and measured using the following EPR parameters: sweep width, 60 G; modulation amplitude, 0.7 G; microwave power, 20 mW; time constant, 0.16 s; receiver gain, 6.3×10^4 ; scan rate, 21.46 G/min. The bars represent 10,000 arbitrary units; (b) Same as in (a), except that SOD (100 U/mL) was added; (c) Same as in (a), except that *cis*-3,5-EDPO (20 mM) was used. EPR parameters: sweep width, 60 G; modulation amplitude, 0.7 G; microwave power, 20 mW; time constant, 0.08 s; receiver gain, 1×10^5 ; scan rate, 42.9 G/min; (d) same as in (a), except that *cis/trans*-4,5-EDPO (20 mM) was used. EPR parameters: sweep width, 60 G; modulation amplitude, 0.7 G; microwave power, 20 mW; time constant, 0.16 s; receiver gain, 1×10^5 ; scan rate, 21.46 G/min. The species marked “*” was not detected when KO_2 was used instead of Xa/XOD.

of 3,5-DPPO and 3,5-DIPPO could, however, only be isolated in minor amounts. 4,5-EDPO consisted of 21% *cis*- and 79% *trans*-isomer (NMR), which could not be separated by conventional chromatographic procedures. In Fig. 2(d) the spectrum obtained from 4,5-EDPO is shown, recorded under conditions identical to those in Fig. 2(a). One species ($a^{\text{N}} = 13.48 \text{ G}$; $a^{\text{H}} = 15.97 \text{ G}$; marked “*”) was not detected in the KO_2 system and is therefore not listed in Table 5.

As already shown above for 3,5-EDPO, no signals were detected in control experiments in which SOD had been added to the incubation mixture prior to xanthine/xanthine oxidase (data not shown).

Half-lives of the respective superoxide adducts were determined as follows: the respective spin traps (40 mM, final concentration) were incubated in water in the presence of ca. 0.5 mg solid KO_2 for 15 s, after which the solution was diluted 1:1 with phosphate buffer (300 mM,

Table 4
Half-life of the superoxide adducts and *n*-octanol/buffer partition coefficients of the spin traps

compound	Apparent $t_{1/2}$ (min)	Partition coefficient <i>n</i> -octanol/phosphate buffer (100 mM, pH 7)
EMPO ^a	8.6	0.15
<i>cis</i> -3,5EDPO	11.5	0.45
<i>trans</i> -3,5EDPO	44.2	0.46
4,5EDPO ^b	44.6	0.44
<i>trans</i> -3,5DPPO	47.3	1.66
4,5DPPO ^c	47.0	1.36
<i>cis</i> -3,5DIPPO ^d	– ^d	0.90 ^d
<i>trans</i> -3,5DIPPO	55.0	1.12
4,5DIPPO ^e	42.8	1.03

^a Data from Stolze et al. [7].

^b *cis/trans* = 21/79.

^c *cis/trans* = 29.6/70.4.

^d ca. 95% *cis* form.

^e *cis/trans* = 24/76.

pH 7.0) containing 20 mM DTPA, SOD (100 U/mL), and catalase (250 U/mL). The final pH was 7.4. The decay of the EPR signal was recorded as a series of consecutive spectra until the superoxide-related lines gradually disappeared. After prolonged incubation an increasing amount of the hydroxyl radical adduct was observed (e.g. for *trans*-3,5-EDPO: ca. 15 % after 30 min). The spectral contribution of this secondary spin adduct was subtracted from each individual EPR spectrum before calculating the respective half-life. For all spin traps the resulting intensity decrease of the first line (or set of lines) was approximated by a first-order exponential decay, which was in good agreement with the experimental data. The Pearson correlation coefficient, which characterizes the quality of approximation, was higher than 0.99 for all spin traps investigated. The respective values of apparent superoxide half-lives are listed in Table 4.

Preliminary tests regarding the overall efficiency of the spin traps (combination of rate constant, line width and half-life) revealed that the obtainable spectral intensity (measured after 3 and 15 min incubation with the xanthine/xanthine oxidase system) was higher than with DEPMPO.

3.3. Spin adduct formation with other oxygen-containing radicals

Using a Fenton system in the presence of the spin traps, EPR spectra of the respective hydroxyl radical adducts could be obtained from all investigated spin traps, e.g. from *trans*-3,5-EDPO (Fig. 3(a)), *cis*-3,5-EDPO (Fig. 3(b)), or 4,5-EDPO (Fig. 3(c)). The hydroxyl radical adducts were rather stable, and only minor changes were observed in the EPR spectra during the first 20 min of incubation.

In order to discriminate between the formation of oxygen- and carbon-centered radical adducts from alcohols such as methanol, two simple model systems were chosen:

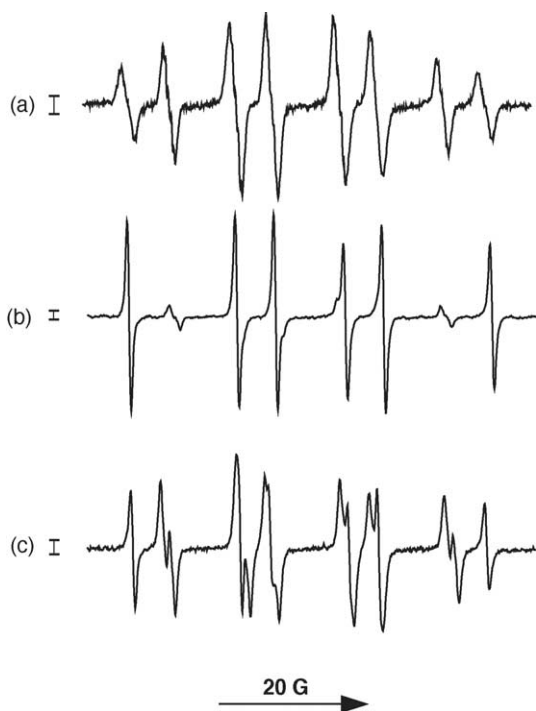


Fig. 3. Formation of the hydroxyl radical adducts of the spin traps *trans*-3,5-EDPO, *cis*-3,5-EDPO, and *cis/trans*-4,5-EDPO; (a) *trans*-3,5-EDPO (20 mM) was incubated with a Fenton system containing FeSO_4 (0.8 mM), EDTA (2 mM), H_2O_2 (0.2%) and the reaction was stopped after 10 s by 1:1 dilution with phosphate buffer (300 mM, pH 7.4, containing 20 mM DTPA) and the spectrum was recorded using the following spectrometer settings: sweep width, 60 G; modulation amplitude, 0.1 G; microwave power, 20 mW; time constant, 0.81 s; receiver gain, 5×10^4 ; scan rate, 42.9 G/min. The bars represent 10,000 arbitrary units; (b) same conditions, except that *cis*-3,5-EDPO was used. EPR parameters: sweep width, 60 G; modulation amplitude, 0.1 G; microwave power, 2 mW; time constant, 0.82 s; receiver gain, 5×10^4 ; scan rate, 42.9 G/min. The bars represent 10,000 arbitrary units; (c) same conditions, except that *cis/trans*-4,5-EDPO was used. EPR parameters: sweep width, 60 G; modulation amplitude, 0.1 G; microwave power, 0.2 mW; time constant, 0.82 s; receiver gain, 5×10^4 ; scan rate, 42.9 G/min. The bars represent 10,000 arbitrary units.

(a) the Fe^{3+} -catalyzed formation of alkoxy radical adducts according to Dikalov and Mason [11] and (b) the α -hydroxymethyl radical generating Fenton system in the presence of 5% methanol according to Roubaud et al. [15].

The first system (Fe^{3+} /methanol [11]) lead to a mixture of two diastereomeric forms of *trans*-3,5-EDPO/ $\bullet\text{OCH}_3$ (Fig. 4(a)), from which the spectrum of the less stable species (Fig. 4(b), marked “**”) was obtained by mathematical subtraction of the succeeding scan (recorded after 6 min) from the first scan shown in Fig. 4(a). In Fig. 4(c), the EPR spectrum obtained from the two diastereomeric forms of *cis*-3,5-EDPO/ $\bullet\text{OCH}_3$ are shown, recorded under otherwise identical conditions. Upon prolonged incubation the methoxyl radical adduct gradually disappeared and increasing amounts of the more stable carbon-centered hydroxymethyl radical adduct were detected, leading to very complex spectra (not shown). The HFS values of the *trans*-3,5-EDPO/ $\bullet\text{CH}_2\text{OH}$ ($a^{\text{N}} = 14.73$ G; $a^{\text{H}} = 17.10$ G; 64% and $a^{\text{N}} = 14.90$ G; $a^{\text{H}} = 24.33$ G; 36%) are, however,

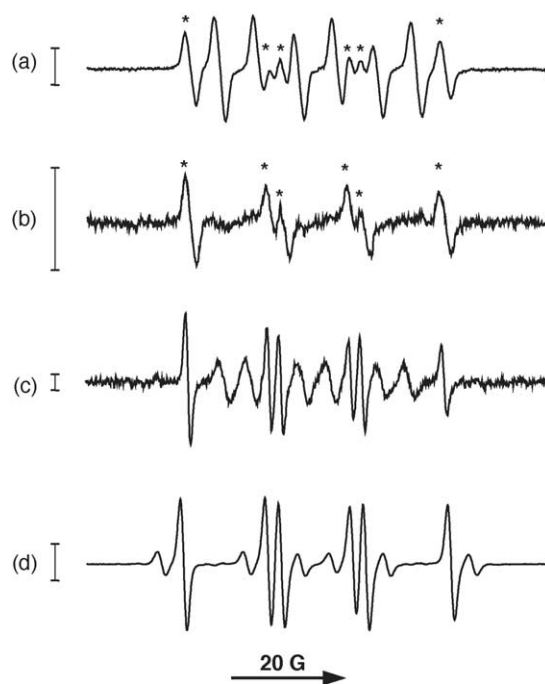


Fig. 4. Methanol-derived oxygen- and carbon-centered spin adducts from the spin traps *trans*- and *cis*-3,5-EDPO; (a) after a 2 min incubation of *trans*-3,5-EDPO (1 M in methanol) with FeCl_3 (10 mM), the reaction was stopped by 1:20 dilution with phosphate buffer (0.15 M, pH 7.4, containing 10 mM DTPA), and the spectrum was recorded with the following spectrometer settings: sweep width, 80 G; modulation amplitude, 0.1 G; microwave power, 20 mW; time constant, 0.08 s; receiver gain, 1×10^5 ; scan rate, 57 G/min. The bars represent 10,000 arbitrary units; (b) difference spectrum between two succeeding scans, clearly showing the minor species (marked “**”) in (a); (c) same conditions as in (a), except that *cis*-3,5-EDPO was used; (d) *trans*-3,5-EDPO (20 mM) was incubated with a Fenton system containing FeSO_4 (1 mM), methanol (10%), EDTA (2 mM), H_2O_2 (0.2%) and the reaction was stopped after 10 s by 1:1 dilution with phosphate buffer (300 mM, pH 7.4, containing 20 mM DTPA). The spectrum was recorded using the following spectrometer settings: sweep width, 80 G; modulation amplitude, 0.24 G; microwave power, 20 mW; time constant, 0.08 s; receiver gain, 1×10^4 ; scan rate, 57 G/min. The bars represent 10,000 arbitrary units.

clearly different from those of the methoxyl radical adduct mentioned above ($a^{\text{N}} = 13.55$ G; $a^{\text{H}} = 6.77$ G; $a^{\text{H}} = 0.99$ G; 61% and $a^{\text{N}} = 13.95$ G; $a^{\text{H}} = 16.10$ G; $a^{\text{H}} = 0.95$ G; 39%). This can be seen in Fig. 4(d), where a Fenton system in the presence of methanol [15] was used to generate an almost pure EPR spectrum of the two diastereomeric forms of the *trans*-3,5-EDPO/ $\bullet\text{CH}_2\text{OH}$ adduct. The spectral contribution of the different species (see Table 5) was assessed by computer simulation (Bruker WINEPR SimFonia).

3.4. Spin trapping of lipid-derived free radicals

Radicals derived from linoleic acid by lipid peroxidation-type processes were also investigated. Radicals were formed in a Fenton-type reaction from peroxidized linoleic acid in the presence of Fe^{2+} [9,10]. An anaerobic setup, obtained by flushing with nitrogen for several minutes, was chosen. The reaction system consisted of peroxidized

Table 5
Comparison of the EPR parameters of different radical adducts of various EMPO derivatives

Radical	HFS (G)	EMPO	c-3,5EDPO		t-3,5EDPO		4,5EDPO		t-3,5DPPO		4,5DPPO		c-3,5DIPPO		t-3,5DIPPO		4,5DIPPO					
•OOH		(57%)	(43%)	(69%)	(31%)	(100%)	–	(36%)	(35%)	(29%) ^a	(100%)	(44%)	(35%)	(21%)	(76%)	(34%)	(100%)	(35%)	(33%)	(32%)		
	<i>a</i> ^N	13.28	13.28	13.50	13.55	13.13	–	13.48	13.48	13.48	13.15	13.49	13.49	13.49	13.15	13.45	13.22	13.48	13.48	13.43		
	<i>a</i> ^H	11.89	9.67	15.40	5.98	8.40	–	9.10	11.60	8.55	8.48	9.25	11.40	6.75	8.18	15.36	8.48	9.70	11.73	7.45		
	<i>a</i> ^H	–	–	–	–	0.90	–	–	–	1.90	–	–	–	–	–	–	–	–	–	–		
•OH		(50%)	(50%)	(67%)	(33%)	(67%)	(33%)	(75%)	(25%)	(86%)	(14%)	(80%)	(20%)	(62%)	(38%)	(85%)	(15%)	(66%)	(34%)			
	<i>a</i> ^N	14.00	14.00	14.50	13.90	13.85	14.30	14.00	14.45	13.85	14.30	13.96	14.45	14.53	13.92	13.85	14.30	13.98	14.47			
	<i>a</i> ^H	15.00	12.58	19.67	8.57	9.00	19.30	10.00	18.60	9.05	19.30	9.92	18.58	19.57	8.80	9.08	19.55	10.07	18.52			
	<i>a</i> ^H	0.90	–	–	0.75	0.75	0.95	1.05	–	0.75	0.95	1.11	–	–	0.75	0.75	0.95	1.11	–			
•H		(100%)		(100%)		(100%)		(100%)		(100%)		(100%)		(100%)		(100%)		(100%)				
	<i>a</i> ^N	15.52		15.52		15.45		15.57		15.42		15.51		15.61		15.46		15.59				
	<i>a</i> ^H	22.21		25.96		25.87		25.31		25.84		25.16		25.90		25.79		25.12				
	<i>a</i> ^H	20.82		16.04		17.50		18.03		17.53		17.82		16.20		17.65		17.96				
•CH ₃		(100%)		(52%)	(48%)	(89%)	(11%)	(98%)	(2%)	(89%)	(11%)	(98%)	(2%)	(52%)	(48%)	(88%)	(12%)	(95%)	(5%)			
	<i>a</i> ^N	15.42		15.45	15.35	15.32	15.35	15.40	15.50	15.31	15.30	15.35	15.35	15.40	15.50	15.35	15.35	15.37	15.48			
	<i>a</i> ^H	22.30		27.00	16.60	16.74	26.20	18.43	26.73	16.69	26.22	18.26	26.70	16.45	27.08	16.82	26.25	18.61	26.52			
•OCH ₃		(50%)	(50%)	(60%)	(40%)	(61%)	(39%) ^b	(56%)	(24%)	(20%)	(56%)	(44%)	(47%)	(29%)	(24%)	(72%)	(28%)	(50%)	(50%)	(44%)	(30%)	(26%)
	<i>a</i> ^N	13.74	13.74	13.62	14.07	13.55	13.95	13.57	13.52	14.13	13.55	13.95	13.65	13.57	14.08	13.68	13.99	13.62	13.95	13.57	13.57	14.10
	<i>a</i> ^H	10.87	7.81	4.60	16.06	6.77	16.10	8.55	4.50	16.43	6.70	16.01	8.30	4.30	16.37	4.93	15.73	6.65	15.90	8.25	4.10	16.25
	<i>a</i> ^H	–	–	–	–	0.99	0.95	0.70	–	–	0.99	0.95	0.70	–	–	–	0.90	0.90	0.70	–	–	
•CH ₂ OH		(100%)		(79%)	(21%)	(64%)	(36%)	(98%)	(2%)	(65%)	(35%)	(98%)	(2%)	(76%)	(24%)	(72%)	(28%)	(96%)	(4%)			
	<i>a</i> ^N	14.95		15.03	15.00	14.73	14.90	15.00	15.00	14.78	14.94	15.00	15.02	15.08	14.95	14.84	14.97	15.00	15.02			
	<i>a</i> ^H	21.25		25.41	16.00	17.10	24.33	18.20	25.30	17.07	24.53	18.02	25.10	25.31	16.04	17.18	24.58	18.05	25.26			
		–		0.50 ³	0.50 ³	–	–	–	–	–	–	–	–	–	0.51 ³	0.50 ³	–	–	–	–		
•C (LOOH)		(62%)	(38%)	(80%)	(10%)	(50%)	(45%)	(68%)	(32%)	(45%)	(45%) ^c	(63%)	(37%)	(38%)	(28%)	(64%)	(24%)	(12%)	(58%)	(42%)		
	<i>a</i> ^N	13.45	13.45	14.45	15.30	14.40	13.75	13.85	14.60	13.79	14.20	13.85	14.58	14.45	15.35	14.30	13.64	14.40	13.85	14.65		
	<i>a</i> ^H	11.45	8.55	19.67	24.20	18.90	8.83	9.90	18.30	8.82	18.90	9.94	18.18	19.60	24.30	19.55	8.82	15.50	10.20	18.20		
	<i>a</i> ^H	–	–	–	–	–	–	1.05	–	–	–	1.10	–	–	–	0.95	–	–	1.10	–		
	–	–	(16.70/8.95) ^d	(15.30/23.00) ^d										(15.40/11.55)								
	–	–	(12.90/10.45) ^d	(15.70/13.70) ^d	–	–	–	–	–	–	–	–	–	(12.90/10.50) ^d	–	–	–	–	–			

^a Fourth species only detected in the Xa/XOD system (*a*^N = 13.48 G; *a*^H = 15.97 G).

^b Data from difference spectrum.

^c Rest mainly •OH-adduct.

^d Approximate values of secondary products.

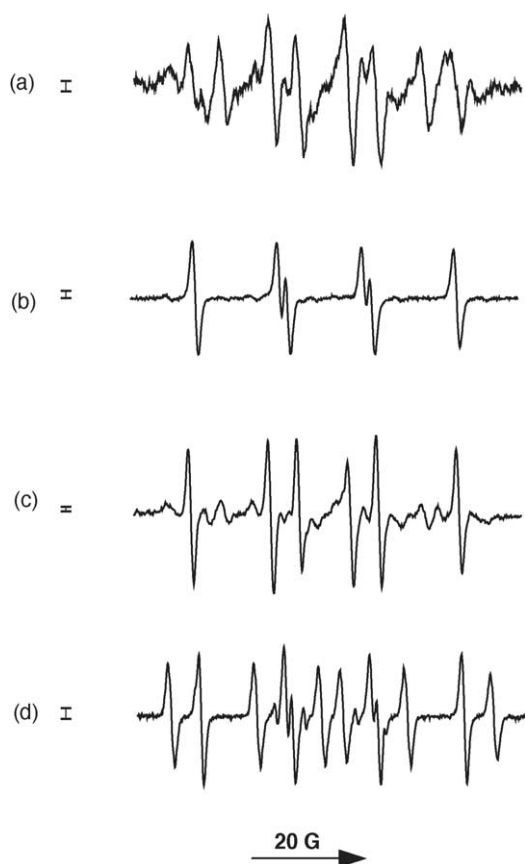


Fig. 5. Lipid-derived radical adducts from peroxidized linoleic acid using a Fenton-type incubation system in the presence of the spin traps *cis*- and *trans*-3,5-EDPO. Comparison with a methyl radical generating model system; (a) to a nitrogen-bubbled solution of peroxidized linoleic acid (2 mM) and *trans*-3,5-EDPO (20 mM) in phosphate buffer (20 mM, pH 7.4, containing 1.5% acetonitrile) FeSO_4 (0.2 mM) was added and the spectrum was recorded with the following spectrometer settings: sweep width, 80 G; modulation amplitude, 1.42 G; microwave power, 20 mW; time constant, 0.16 s; receiver gain, 1×10^6 ; scan rate, 57.27 G/min. 5 Scans accumulated. The bars represent 10,000 arbitrary units; (b) *trans*-3,5-EDPO (20 mM) was incubated with a Fenton system containing FeSO_4 (1 mM), DMSO (10%), EDTA (2 mM), H_2O_2 (0.2%) and the reaction was stopped after 10 s by 1:1 dilution with phosphate buffer (300 mM, pH 7.4, containing 20 mM DTPA). The spectrum was recorded using the following spectrometer settings: sweep width, 70 G; modulation amplitude, 0.1 G; microwave power, 20 mW; time constant, 0.16 s; receiver gain, 5×10^5 ; scan rate, 25.03 G/min. The bars represent 10,000 arbitrary units; (c) same conditions as in a), except that *cis*-3,5-EDPO (20 mM) was used; (d) same conditions as in (b), except that *cis*-3,5-EDPO (20 mM) was used.

linoleic acid and the respective spin trap dissolved in 20 mM phosphate buffer, pH 7.4, containing 1.5% acetonitrile. To this solution Fe^{2+} , dissolved in nitrogen-purged water, was added in order to start the formation of free radicals, as recently tested with different derivatives of DEPMPO [9,10], EMPO [7], Trazon [12] or EPPN [16,17]. In Fig. 5(a), the EPR spectrum obtained from *trans*-3,5-EDPO is shown, consisting of four different species, one of which was identified as the hydroxyl radical adduct (see above, Fig. 3(a)). For comparison, a typical carbon-centered radical adduct (*trans*-3,5-EDPO/ $\bullet\text{CH}_3$), generated in a Fenton-type model system in the presence of DMSO can

be seen in Fig. 5(b). The respective experiments performed with *cis*-3,5-EDPO can be seen in Fig. 5(c) (*cis*-3,5-EDPO/LOOH/ Fe^{2+}) and Fig. 5d (*cis*-3,5-EDPO/ $\bullet\text{CH}_3$). Comparison with data from Table 5 makes the contribution of the hydroxyl radical adduct ($a^{\text{N}} = 14.45$ G; $a^{\text{H}} = 19.67$ G; 80%, see also above, Fig. 3(b)) as well as a carbon-centered radical adduct ($a^{\text{N}} = 15.30$ G; $a^{\text{H}} = 24.20$ G; 10%) likely. The spectral parameters of lipid-derived adducts of the other spin traps are listed in Table 5.

4. Discussion

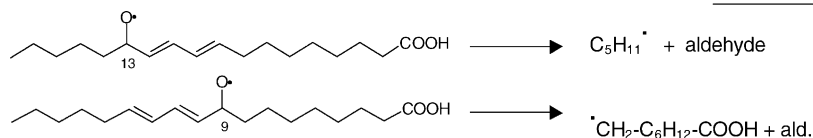
Several novel compounds derived from the spin trap EMPO with an extra methyl group in position 3 or 4 of the pyrroline ring were synthesized and fully characterized in this study. Complete ^1H and ^{13}C signal assignment was performed.

The substances form very stable superoxide adducts ($t_{1/2} = \text{ca. } 12\text{--}55$ min), which are at least 15 times more stable than the respective adducts with DMPO ($t_{1/2} = 45$ s) [4]. The stabilities of the superoxide adducts of *trans*-3,5-EDPO, *trans*-DPPO and *trans*-DIPPO even exceed those of the EMPO derivatives iPrMPO or sBuMPO ($t_{1/2} > 20$ min [1]) or DEPMPO and its derivatives ($t_{1/2} = \text{ca. } 7\text{--}15$ min [8–10]).

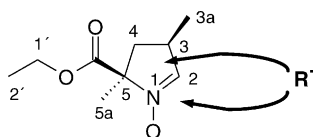
The half-lives of the superoxide adducts were determined according to a first-order exponential decay approximation (Pearson correlation coefficient $r^2 > 0.99$). Under the experimental conditions used a second order decay of the superoxide adducts was negligible. An important aspect to consider is the fact that the observed spectral intensity does not only depend on the half-life of the spin adducts, but also on the rate constant of the spin trapping reaction, the spectral line width, and the total number of lines, and additional factors, such as enzyme binding or the solubility (aggregate formation) of the spin trap. Preliminary tests, based on the spectral intensity of the respective superoxide spin adducts after 3 and 15 min, have shown that the performance of the investigated spin traps is almost two-fold higher than with DEPMPO, increasing with incubation time due to its higher stability.

All novel compounds formed hydroxyl and methoxyl radical adducts. Whereas hydroxyl radical adducts were quite stable, the respective methoxyl radical adducts gradually disappeared and the more stable hydroxymethyl radical adducts became the predominant species. Several radicals adducts were formed from peroxidized linoleic acid, the major component being the hydroxyl radical adduct possibly formed according to secondary reactions or iron-catalyzed hydrolysis of the spin trap. Secondary product formation from $\text{LOO}\bullet$ and $\text{LO}\bullet$ has also been reported by other authors [18–24]. The structure of various secondary radical adducts could not be determined, but the oxygen in the initially formed alkoxy radical formed from peroxidized linoleic acid is most likely situated at position

9 or 13. Before trapping these very short-lived species undergo rapid β -scission [25,26] leading to secondary carbon-centered radical species such as the pentyl radical or the octanoic acid radical, from which stable spin adducts can be expected.



The investigated spin traps possess two chiral centers within the molecule (located at the positions of the methyl groups (3 and 5 or 4 and 5)). Only 3,5-EDPO could be fully separated into two pure diastereomers by column chromatography. Upon reaction with the attacking radical a third chiral center is formed, as the radical can attack the pyrroline ring from two sides:



In some cases only one product was detected in the EPR spectrum, which indicates significant differences in reaction rate and adduct stability. Otherwise, a superimposed spectrum was observed which had to be deconvoluted mathematically. In the case of the respective *trans*-3,5-isomers, exceptionally stable superoxide adducts were observed with half-lives ranging from about 44–55 min. These spin traps can therefore be recommended for superoxide trapping. Additional studies in biological systems including cytotoxicity tests with various cell lines will follow in the near future.

Acknowledgements

The authors would like to thank R. Stadtmüller and A. Hofinger for skilful technical assistance in synthesis, purification, and characterization of the spin traps. The present study was supported by the Austrian Fonds zur Förderung der wissenschaftlichen Forschung.

References

- [1] Stolze K, Udilova N, Rosenau T, Hofinger A, Nohl H. Synthesis and characterization of EMPO-derived 5,5-disubstituted 1-pyrroline *N*-oxides as spin traps forming exceptionally stable superoxide spin adducts. *Biol Chem* 2003;384:493–500.
- [2] Zhao H, Joseph J, Zhang H, Karoui H, Kalyanaraman B. Synthesis and biochemical applications of a solid cyclic nitron spin trap: A relatively superior trap for detecting superoxide anions and glutathyl radicals. *Free Rad Biol Med* 2001;31:599–606.

- [3] Tsai P, Ichikawa K, Mailer C, Pou S, Halpern HJ, Robinson BH, et al. Esters of 5-carboxyl-5-methyl-1-pyrroline *N*-oxide: A family of spin traps for superoxide. *J Org Chem* 2003;68:7811–7.
- [4] Buettner GR, Oberley LW. Considerations in the spin trapping of superoxide and hydroxyl radical in aqueous systems using 5,5-dimethyl-1-pyrroline-1-oxide. *Biochem Biophys Res Commun* 1978;83:69–74.

- [5] Olive G, Mercier A, LeMoigne F, Rockenbauer A, Tordo P. 2-Ethoxycarbonyl-2-methyl-3,4-dihydro-2H-pyrrole-1-oxide: Evaluation of the spin trapping properties. *Free Radic Biol Med* 2000;28:403–8.
- [6] Zhang H, Joseph J, Vasquez-Vivar J, Karoui H, Nsanzumuhire C, Martásek P, et al. Detection of superoxide anion using an isotopically labeled nitron spin trap: Potential biological applications. *FEBS Lett* 2000;473:58–62.
- [7] Stolze K, Udilova N, Nohl H. Spin adducts of superoxide, alkoxyl, and lipid-derived radicals with EMPO and its derivatives. *Biol Chem* 2002;383:813–20.
- [8] Fréjaville C, Karoui H, Tuccio B, Le Moigne F, Culcasi M, Pietri S, et al. 5-(Diethoxyphosphoryl)-5-methyl-1-pyrroline *N*-oxide: A new efficient phosphorylated nitron for the *in vitro* and *in vivo* spin trapping of oxygen-centered radicals. *J Med Chem* 1995;38:258–65.
- [9] Stolze K, Udilova N, Nohl H. Spin trapping of lipid radicals with DEPMPO-derived spin traps: Detection of superoxide, alkyl and alkoxyl radicals in aqueous and lipid phase. *Free Radic Biol Med* 2000;29:1005–14.
- [10] Stolze K, Udilova N, Nohl H. Lipid radicals: Properties and detection by spin trapping. *Acta Biochim Polonica* 2000;47:923–30.
- [11] Dikalov SI, Mason RP. Spin trapping of polyunsaturated fatty acid-derived peroxy radicals: Reassignment to alkoxyl radical adducts. *Free Radic Biol Med* 2001;30:187–97.
- [12] Stolze K, Udilova N, Nohl H. ESR analysis of spin adducts of alkoxyl and lipid-derived radicals with the spin trap Trazon. *Biochem Pharmacol* 2002;63:1465–70.
- [13] Sankuratri N, Janzen EG. Synthesis and spin trapping chemistry of a novel bicyclic nitron: 13,3-trimethyl-6-azabicyclo[3.2.1]oct-6-ene-*N*-oxide (Trazon). *Tetrahedron Lett* 1996;37:5313–6.
- [14] O'Brien PJ. Intracellular mechanisms for the decomposition of a lipid peroxide. I. Decomposition of a lipid peroxide by metal ions, heme compounds, and nucleophiles. *Can J Biochem* 1969;47:485–92.
- [15] Roubaud V, Lauricella R, Bouteiller JC, Tuccio B. *N*-2-(2-Ethoxycarbonyl-propyl)- α -phenylnitron: An efficacious lipophilic spin trap for superoxide detection. *Arch Biochem Biophys* 2002;397:51–6.
- [16] Stolze K, Udilova N, Rosenau T, Hofinger A, Nohl H. Spin trapping of superoxide, alkyl- and lipid-derived radicals with derivatives of the spin trap EPPN. *Biochem Pharmacol* 2003;66:1717–26.
- [17] Stolze K, Udilova N, Rosenau T, Hofinger A, Nohl H. Spin adducts of several *N*-2-(2-alkoxycarbonyl-propyl)- α -pyridylnitron derivatives with superoxide, alkyl and lipid-derived radicals. *Biochem Pharmacol* 2004;68:185–93.
- [18] Rota C, Barr DP, Martin MV, Guengerich FP, Tomasi A, Mason RP. Detection of free radicals produced from the reaction of cytochrome P-450 with linoleic acid hydroperoxide. *Biochem J* 1997;328:565–71.
- [19] Van der Zee J, Barr DP, Mason RP. ESR spin trapping investigation of radical formation from the reaction between hematin and tert-butyl hydroperoxide. *Free Radic Biol Med* 1996;20:199–206.
- [20] Akaike T, Sato K, Ijiri S, Miyamoto Y, Kohno M, Ando M, et al. Bactericidal activity of alkyl peroxy radicals generated by heme-iron-catalyzed decomposition of organic peroxides. *Arch Biochem Biophys* 1992;294:55–63.

- [21] Kalyanaraman B, Mottley C, Mason RP. A direct ESR and spin-trapping investigation of peroxy free radical formation by hematin/hydroperoxide systems. *J Biol Chem* 1983;258:3855–8.
- [22] Chamulitrat W, Takahashi N, Mason RP. Peroxy, alkoxy, and carbon-centered radical formation from organic hydroperoxides by chloroperoxidase. *J Biol Chem* 1989;264:7889–99.
- [23] Davies MJ. Detection of peroxy and alkoxy radicals produced by reaction of hydroperoxides with heme-proteins by ESR spectroscopy. *Biochim Biophys Acta* 1988;964:28–35.
- [24] Davies MJ. Detection of peroxy and alkoxy radicals produced by reaction of hydroperoxides with rat liver microsomal fractions. *Biochem J* 1989;257:603–6.
- [25] Iwahashi H, Deterding LJ, Parker CE, Mason RP, Tomer KB. Identification of radical adducts formed in the reactions of unsaturated fatty acids with soybean lipoxygenase using continuous flow fast atom bombardment with tandem mass spectrometry. *Free Rad Res* 1996;25:255–74.
- [26] Dikalov SI, Mason RP. Reassignment of organic peroxy radical adducts. *Free Radic Biol Med* 1999;27:864–72.